



HHS Public Access

Author manuscript

Atherosclerosis. Author manuscript; available in PMC 2020 September 25.

Published in final edited form as:

Atherosclerosis. 2014 September ; 236(1): 121–130. doi:10.1016/j.atherosclerosis.2014.06.015.

Hepatic overexpression of the prodomain of furin lessens progression of atherosclerosis and reduces vascular remodeling in response to injury

Xia Lei¹, Debapriya Basu¹, Zhiqiang Li¹, Maoxiang Zhang², R. Dan Rudic², Xian-Cheng Jiang¹, Weijun Jin¹

¹Department of Cell Biology, State University of New York, Downstate Medical Center, Brooklyn, NY, 11203

²Department of Pharmacology, Georgia Regents University, Augusta, GA 30912

Abstract

Atherosclerosis is a complex disease, involving elevated LDL-c levels, lipid accumulation in the blood vessel wall, foam cell formation and vascular dysfunction. Lowering plasma LDL-c levels is the cornerstone of current management of cardiovascular disease. However, new approaches that can reduce plasma LDL-c levels and lessen the pathological vascular remodeling that occurs in the disease should also have therapeutic value. Previously, we found that over-expression of profurin, the 83-amino acid prodomain of the proprotein convertase furin, lowered plasma HDL levels in wild-type mice. The question that remained was whether it had effects on apolipoprotein B (ApoB)-containing lipoproteins. In this study, we evaluated profurin for effects on ApoB-containing lipoproteins, atherosclerosis and vascular remodeling *in vivo*. Hepatic profurin overexpression resulted in a significant reduction in atherosclerotic lesion development in *Ldlr*^{-/-} mice and a robust reduction in plasma LDL-c levels. Metabolic studies revealed that the secretion of ApoB and triglycerides in VLDL particles was greatly reduced. Mechanistic studies showed that in the presence of profurin, hepatic ApoB, mainly ApoB100, was degraded by proteasomes. There was no effect on ApoB mRNA expression. Importantly, short-term hepatic profurin overexpression did not result in hepatic lipid accumulation. Blood vessel wall thickening caused by either wire-induced femoral artery injury or common carotid artery ligation was reduced. When expressed in vascular smooth muscle cells *in vitro*, profurin inhibited proliferation and migration. These results indicate that a profurin-based therapy has the potential to treat atherosclerosis by improving metabolic lipid profiles and reducing both atherosclerotic lesion development and pathological vascular remodeling.

Correspondence: Weijun Jin, M.D., Department of Cell Biology, MSC #2, SUNY Downstate Medical Center, 450 Clarkson Avenue, Brooklyn, NY, 11203, Tel: 718-221-5639, Fax: 718-270-3732, weijun.jin@downstate.edu.

Publisher's Disclaimer: This is a PDF file of an unedited manuscript that has been accepted for publication. As a service to our customers we are providing this early version of the manuscript. The manuscript will undergo copyediting, typesetting, and review of the resulting proof before it is published in its final citable form. Please note that during the production process errors may be discovered which could affect the content, and all legal disclaimers that apply to the journal pertain.

Introduction

Proprotein convertases (PCSKs) constitute a family of calcium-dependent serine endopeptidases that are conserved from bacteria to mammals. Of the nine members, all except two are known as the “typical proprotein convertases (TPCs)” and activate (or inactivate, depending on the substrate) peptides/proteins by cleaving after the final basic residue of the peptide (R/K)-Xn-(R/K)¹. PCSK9 and S1P are atypical in that they cleave following non-basic residues².

Hepatic PCSK9 and S1P have established roles in plasma lipid metabolism³. However, the roles of the other hepatic TPCs in lipid metabolism are unclear. Because all except PCSK1, 2 and 4 are expressed in the liver and there is considerable overlap in their substrates, it is difficult to study their individual roles in lipid metabolism². The situation is further complicated in that global knockout of each TPC is lethal².

The TPCs, including those expressed in the liver, are synthesized as inactive zymogens in the endoplasmic reticulum. Each contains an N-terminal prodomain that is presumed to act as both a specific intramolecular chaperone and an inhibitor of the convertase’s proteolytic activity. Profurin, an 83-amino-acid peptide, is the prodomain of furin (PCSK3) and is generated during the passage of furin from the endoplasmic reticulum to the Golgi. Endogenous profurin undergoes rapid intracellular degradation after assisting in furin maturation⁴. However, when overexpressed, profurin is one of the most potent TPC catalytic site inhibitors and has been shown by several groups, including ours^{5, 6}, to inhibit the activity of multiple TPCs both *in vitro* and *in vivo*. Previously, we found that hepatic overexpression of profurin dramatically reduced plasma HDL levels⁶. However, the effect of profurin overexpression on lipid metabolism beyond that on HDL remained to be determined.

There are few studies directly demonstrating a role for the TPCs in atherosclerosis. The most compelling comes from the observation that furin and PCSK5 are expressed in human atherosclerotic lesions and that their expression is up-regulated following vascular injury *in vivo* in animal models⁷. It was therefore of interest to determine whether profurin, the TPCs’ inhibitor, had any significant impact on vascular disease.

Here we describe the effects of overexpression of profurin on apolipoprotein B (apo-B) containing lipoproteins, atherosclerosis, and vascular remodeling in response to injury. We find that hepatic profurin overexpression *in vivo* robustly lowers plasma LDL-c levels and is vasculoprotective.

Methods

Adenoviral Vectors

Adenovirus encoding human profurin (Ad-profurin) and control adenovirus without a transgenic expression cassette (Ad-null) were generated as previously described⁸.

Mice and Diets

Wild-type (WT) and *Ldlr*^{-/-} mice (8-week-old females) on a C57BL/6J background were purchased from Jackson Laboratory (Bar Harbor, ME). All procedures were conducted in conformity with the United States Public Health Service Policy on Humane Care and Use of Laboratory Animals and approved by the Institutional Animal Care and Use Committee of SUNY Downstate Medical Center. Plasma samples were collected on the third day after virus injection. Mice were fed a chow diet unless otherwise stated in the text. For the time course study of Fig. 4, *Ldlr*^{-/-} mice were injected with Ad-null or Ad-profurin (10¹¹ viral particles/mouse) via the tail vein (n=4 in each group). Plasma samples were collected on days 0, 3, 5, 14 and 28 after injection. For the atherosclerosis study of Fig. 1, *Ldlr*^{-/-} mice were fed a Western diet (TD88137; Harlan Teklad, Madison, WI) for 4 weeks. They were then divided into two groups (n=11 in each group), injected with Ad-null or Ad-profurin (10¹¹ particles/mouse) via the tail vein (day 0) and subsequently fed the Western diet for another 4 weeks (Day 28). Finally, they were sacrificed after 4 hours of fasting. Plasma and liver samples were collected, and atherosclerotic lesions were analyzed as described⁹. Experimental details regarding diet and sample timing for other experiments are given in the text and Fig. legends.

Lipid Analysis

For blood sampling, mice were fasted for 4 hours and bled from the retro-orbital plexus under isoflurane anesthesia using heparinized microcapillary tubes. Blood was centrifuged at 10,000 × g for 10 min at 4°C and plasma was separated and used for the analysis and/or stored at -70°C. Liver lipid was extracted using the Folch method¹⁰. Total triglyceride, cholesterol, phospholipids and HDL cholesterol were determined using commercially available kits (Wako Pure Chemical Industries Ltd, Richmond, VA.). ApoB-containing lipoprotein cholesterol was calculated by subtracting HDL cholesterol from total cholesterol. Lipoprotein profiles were obtained from equal amounts of pooled plasma samples of the mice constituting experimental groups by fast-protein liquid chromatography (FPLC) as described¹¹.

Atherosclerotic Lesion Measurement

Mice were fasted for 4 hours and then sacrificed under anesthesia. The aorta was dissected *in situ* from the ascending aorta to the iliac bifurcation and the arch photographed. An aortic root assay and an *en face* assay were performed as previously described⁹. Briefly, the heart was removed with the ascending aorta cut halfway between the aortic root and the brachiocephalic artery. The aortic root was sectioned horizontally into 10 μm-thick slices which were stained with hematoxylin and eosin. Total intimal lesion area and acellular/anuclear areas (negative for hematoxylin-positive nuclei) per total cross section area were quantified by taking the average of 6 sections spaced 30 μm apart, beginning at the base of the aortic root. The results were expressed as the average for the 6 sections. For the *en face* assay, the dissected aorta from the arch to the iliac bifurcation was opened longitudinally, fixed between glass slides and stained with Oil Red O. The *en face* lesion area of the aorta was quantified relative to total surface area as described⁹. Images were viewed and captured with a Nikon Labophot 2 microscope equipped with a SPOT RT3 color video camera

attached to a computerized imaging system with Image-Pro Plus version 6.0 software (Media Cybernetics Inc. Rockville, MD). Macrophage and trichrome staining were carried out as previously reported ¹².

Femoral Artery Injury and Flow Dependent Vascular Remodeling

Adenoviral vectors (10^{11} particles/mouse) were intravenously injected immediately prior to artery injury or ligation. Femoral artery injury and left common carotid artery ligation were performed as previously reported ¹³. To induce a denuding endothelial injury, the inside of the left femoral artery of mice was repeatedly scraped (5–7 times) by the end of a straight wire (0.38 mm in diameter, No. C-SF-15-15, Cook, Inc.) inserted into the artery to systematically disrupt the inner lumen of the vessel ¹³. To generate flow dependent vascular remodeling, the distal left common carotid artery (LC) artery and its bifurcation into the external and internal carotid were exposed using blunt dissection. 8-0 nylon sutures (USSC Sutures) were used to ligate the LC artery, just proximal to the external/internal carotid artery bifurcation. Incisions were closed (5-0 suture) and mice were left to recover. After 5 weeks of flow reduction induced by LC ligation and wire injury, mice were anesthetized, exsanguinated, and perfused via the left ventricle with physiologic saline. Mice were subsequently perfusion fixed with neutral buffered formalin. Left femoral arteries and both right and left common carotid arteries were carefully excised and post-fixed either overnight for morphometric studies or immediately embedded in frozen medium for cryotome processing. Morphometric analysis of the carotid arteries was performed using video microscopy as described ¹³. Wall thickness was quantified at 4 regions 90° apart in one location and compared.

Western Blot Analysis

SDS-PAGE employed a 4–20% gradient gel with 0.1 µl of mouse plasma applied per well. The separated proteins were electroblotted to a PVDF membrane and Western blot analysis for mouse ApoB and ApoE and carried out as described ¹⁴ using anti-ApoB and anti-ApoE antibodies (Abs) sc-12332 and sc-31283, respectively (Santa Cruz Biotechnology, Dallas, TX). The anti-profurin antibody was kindly provided by Dr. Nabil G. Seidah and the anti-microsomal triacylglyceride transfer protein (MTP) antibody was a gift from Dr. M. Mahmood Hussain. Liver homogenates or cell lysates were prepared in RIPA buffer with added protease inhibitor cocktail (Sigma, St. Louis, MO). Protein was quantified using the BCA kit (Fisher Scientific, Pittsburgh, PA) and equal amounts of protein (50 µg) were loaded on a 4–20% gel. Anti-profurin and anti-actin Abs were used as previously described¹⁰. Blots were incubated with appropriate horseradish peroxidase-conjugated secondary Abs (Jackson ImmunoResearch, West Grove, PA) followed by detection with a SuperSignal West Pico kit (Fisher Scientific, Pittsburgh, PA). The blots were scanned using a ScanMaker 5950 scanner (MicroTek, Santa Fe Springs, CA) and the intensity of each band measured by Image-Pro Plus version 6.0.

RNA isolation, cDNA synthesis and real-time PCR

RNA was isolated from livers or cells using the GeneJet RNA isolation kit (Thermo Scientific, Waltham, MA). RNA concentration was measured using the Nanodrop 2000 (Thermo Scientific, Waltham, MA) and 1.5 µg RNA per sample was used for cDNA

synthesis using the Verso cDNA kit (Thermo Scientific, Waltham, MA). cDNA was amplified with gene specific primers and detected with the Absolute Blue SYBR Green SYBR Green ROX Mix (Thermo Scientific, Waltham, MA) in the StepOne Plus Realtime PCR machine (Applied Biosystems, Grand Island, NY). 18S RNA was used as an invariant control. The standard curve method of analysis for RNA quantitation was utilized using dilutions of corresponding cDNA plasmids as the standards. The primer sequences for MTP and apoB were obtained from the Primer Bank (<http://pga.mgh.harvard.edu/primerbank/>).

Hepatocyte isolation and culture

primary murine hepatocytes from WT mice were isolated as previously reported⁶. Cells were infected with either Ad-null or Ad-profurin at 1.4×10^9 viral particles/ml. After 48 hours, cell lysates were prepared in RIPA buffer with added protease inhibitor cocktail.

Cell Proliferation, Migration Assay and Flow Cytometry

Vascular smooth muscle cells (VSMCs) were isolated from aortas of WT mice as previously reported¹⁵. Cell proliferation was quantified using the BrdU cell proliferation assay kit (cat. 6813, Cell Signaling, Danvers, MA). Briefly, VSMCs were infected with either Ad-null or Ad-profurin at 1.4×10^9 viral particles/ml. After 48 hours, the VSMCs were plated onto 96-well plates at 5000 cells/well and incubated for 24 hours with media containing 25 ng/mL PDGF and a final concentration of 10 μ M BrdU. BrdU incorporation into VSMCs was assessed with a BrdU cell proliferation ELISA kit.

For cell migration studies, VSMCs were grown to 90% confluence at 37°C in a 5% CO₂ atmosphere, harvested by trypsinization, and washed with DMEM medium. The cells were then re-suspended (10^6 cells/ml) and 100 μ l aliquots were placed in the upper compartments of Transwell chemotaxis inserts (Fisher Scientific, Pittsburgh, PA) where the 8- μ m-pore-size filters had previously been coated with fibronectin (10 μ g per filter) and dried. Inserts were placed upon the lower compartments containing 500 μ l of medium and 25 ng/ml platelet derived growth factor (PDGF, Sigma, St. Louis, MO). After 4 hours of incubation at 37°C in a 5% CO₂ atmosphere, the cells on the upper side of the insert were removed with a cotton swab and the cells that had migrated toward the bottom surface of the filters were fixed with 3.75% formaldehyde and stained with a crystal violet staining solution. Four randomly selected fields (10 x objective) were photographed, and the migrated cells were counted. Quantification was performed by solubilizing stained cells in acetic acid and measuring absorbance at 570nm.

For cell cycle analysis, 1×10^6 VSMCs were incubated with 25 ng/mL PDGF for 24 hours, harvested with trypsin, and stained with 100 μ g/ml propidium iodide for 12 hours in the dark at 4°C. The fractions of cells present in each phase of the cell cycle (G0/G1, S, and G2/M) were determined by flow cytometry using a Becton Dickinson FACStar flow cytometer and Modifit software.

Statistical Analysis

Data are presented as the mean \pm standard deviation (SD). Differences between two groups were analyzed using unpaired Student's *t* tests; $p < 0.05$ was considered to be statistically significant.

Results

Hepatic profurin overexpression reduced atherosclerotic lesion formation in *Ldlr*^{-/-} mice

Since we found previously that hepatic profurin overexpression dramatically reduced plasma HDL levels and prevented reverse cholesterol transport in WT mice⁶, we anticipated that hepatic profurin overexpression would increase atherogenesis. To test this, we followed a protocol that had previously been used to study atherosclerosis in mice following adenovirus-mediated apolipoprotein M gene transfer¹⁶. Female *Ldlr*^{-/-} mice were fed a Western diet for 4 weeks and then transduced with either Ad-profurin or Ad-null as indicated schematically in Fig. S1. The diet was continued for another 4 weeks at which point the mice were sacrificed and atherosclerotic lesion formation evaluated. This diet has previously been shown to induce atherosclerotic lesions in *Ldlr*^{-/-} mice¹².

On day 28 after transduction there was detectable hepatic profurin mRNA expression in only the Ad-profurin transduced mice (Fig. 1A). The effect of profurin overexpression on atherosclerotic lesion size was analyzed at this time. All mice had lesions in the aortic arches. However, contrary to our expectation, the Ad-profurin injected mice had noticeably smaller lesions in the aortic arches than the Ad-null injected mice (Fig. 1B). *En face* Oil Red O staining of the whole aorta showed a significant reduction in lesions in Ad-profurin injected mice compared with Ad-null injected (36% decrease, $P < 0.01$, Fig. 1, C and D). Moreover, a significant reduction in mean proximal aortic lesion area was found using the aortic root assay (45% decrease, $P < 0.01$, Fig. 1, E and F).

To evaluate lesion composition, the aortic root sections were immunostained to determine macrophage levels. Although all sections stained positively for the macrophage marker MOMA, Ad-profurin injected mice had a significant reduction in macrophage content compared with Ad-null injected mice (34% reduction, $P < 0.05$, Fig. 1, G and H). However, collagen staining by Masson trichrome showed no significant differences between the groups (Fig. 1, I and J). In addition, there was no significant difference between the two groups in daily food intake throughout the study period (Fig. S2A), and body weight and liver weight after sacrifice were also similar between the two groups (Fig. S2, B and C).

Taken together, these data show that hepatic profurin overexpression has a notably protective effect on atherosclerotic lesion formation in hypercholesterolemic *Ldlr*^{-/-} mice.

Hepatic profurin overexpression reduced plasma lipid levels in *Ldlr*^{-/-} mice on a Western diet

To investigate how hepatic profurin overexpression reduced lesion formation, we measured plasma lipids in *Ldlr*^{-/-} mice fed the Western diet for 4 weeks and then transduced with either Ad-profurin or Ad-null. The diet was continued and the mice were sacrificed on day 3

after transduction. From previous work using the adenoviral vector in mice⁶, we know that at this time the transgene is highly expressed. Both total cholesterol (TC) (630.5 ± 5.1 vs. 1003.1 ± 5.0 mg/dl, $P < 0.01$) and triglyceride (TG) (75.9 ± 9.5 vs. 259.2 ± 27.8 mg/dl, $P < 0.01$) were reduced in Ad-profurin compared with control *Ldlr*^{-/-} mice (Fig. 2, A and B, respectively). In agreement, FPLC analysis revealed reduction of TG and TC levels in the LDL fractions (Fig. 2, C and 3D, respectively). WT mice carry most of their cholesterol in HDL. In *Ldlr*^{-/-} mice on a Western diet, the HDL-c peak was small compared to the LDL-c peak in both Ad-profurin and Ad-null *Ldlr*^{-/-} mice due to significantly higher LDL-c accumulation (Fig. 2D). However, presence of the HDL peak was confirmed by probing for apoA-I in the FPLC fraction 20–28. Clearly, both cholesterol and apoA-1 levels in fractions 20, 22 and 24 were decreased in Ad-profurin compared with Ad-null *Ldlr*^{-/-} mice (Fig. 2, D and E). The HDL results are in agreement with our previous observation that hepatic profurin overexpression reduces HDL levels in WT mice⁶.

These reductions in LDL lipid levels in Ad-profurin transduced *Ldlr*^{-/-} mice were associated with a 50% reduction in plasma ApoB100 and ApoB 48 protein levels (Fig. 3A, upper panel and 3B). However, there were no statistically significant differences in the plasma ApoE levels of the Ad-profurin and Ad-null transduced groups (Fig. 3A, lower panel).

Transient hepatic profurin overexpression reduced multiple plasma lipid levels for an extended time period in *Ldlr*^{-/-} mice

To examine the duration of the effects of hepatic profurin overexpression on plasma lipids, multiple plasma lipid levels were monitored over a 28-day period in *Ldlr*^{-/-} mice on a chow diet following hepatic transduction. On day 3, hepatic profurin overexpression significantly reduced HDL-c levels (9.5 ± 3.1 vs. 91.8 ± 7.8 mg/dl, $P < 0.05$) and phospholipids (39.0 ± 8.4 vs. 311.3 ± 40.8 mg/dl, $P < 0.05$) in *Ldlr*^{-/-} mice compared with Ad-null transduced *Ldlr*^{-/-} mice (Fig. 4, A and B). Significant reductions were also found in ApoB-containing lipoprotein cholesterol (31.8 ± 10.3 vs. 144.8 ± 31.3 mg/dl, $P < 0.05$) and TG (10.3 ± 1.0 vs. 92.3 ± 17.5 mg/dl, $P < 0.05$) (Fig. 4, C and D). All effects gradually attenuated as a function of post-infection time, lasting approximately three weeks, reflecting the gradual decrease over time in hepatic profurin expression after adenovirus-mediated gene transfer¹⁷.

Hepatic profurin overexpression reduced VLDL secretion

To explore how hepatic profurin overexpression reduced plasma LDL-c and ApoB levels, we studied VLDL secretion in *Ldlr*^{-/-} mice transduced with either Ad-profurin or Ad-null. On day 3 after transduction, overnight fasted mice were injected intraperitoneally with poloxamer 407 (P407) and plasma TG and ApoB levels were monitored over a period of 4h. P407 inhibits lipoprotein lipase, endothelial lipase and hepatic lipase activities, preventing the degradation of plasma TG-rich lipoproteins¹⁸. As shown in Fig. 5A, significantly less TG was secreted in Ad-profurin than in Ad-null animals, even at time 0 for administration of P407. The number of VLDL particles secreted *in vivo* by the liver was also lower in Ad-profurin than in Ad-null mice as indicated by both ApoB48 and ApoB100 levels (Fig. 5B). These findings indicate that hepatic profurin overexpression significantly reduced the secretion of ApoB and TG in VLDL particles. Note: profurin has a greater effect on plasma

ApoB levels in mice on a chow diet than on a Western diet (Fig. 5B, 0 minute, versus Fig. 3A), reflecting the greater contribution of intestinal ApoB in the Western diet.

To gain insight into the molecular mechanism by which profurin reduced VLDL secretion, we analyzed liver mRNA in *Ldlr*^{-/-} mice on day 3 after transduction with Ad-null or Ad-profurin and revealed that the levels of ApoB and MTP mRNA did not differ between the groups (Fig. 6A and B). Analysis of liver lysates by Western blotting confirmed the expression of profurin and showed that ApoB100, and, to a lesser extent ApoB48, were significantly reduced by profurin overexpression (Fig. 6C). However, MTP protein levels were not changed (Fig. 6C). Thus profurin overexpression reduces ApoB100 protein but not mRNA levels, and does not reduce VLDL secretion through effects on MTP.

To demonstrate the effect of profurin on apoB degradation in hepatocytes, primary murine hepatocytes from *Ldlr*^{-/-} mice were isolated and transduced with either Ad-null or Ad-profurin. Profurin treatment reduced the levels of intracellular ApoB100 protein, whereas ApoB48 levels were only slightly decreased (Fig. 6D, lane 2 versus lane 1). The presence of MG132, a specific proteasome inhibitor, prevented the degradation of profurin protein (Fig. 6D, lane 4 versus lane 2). Also MG132 partially blunted the reduction in intracellular levels of ApoB100 in ad-profurin transduced hepatocytes (Fig. 6D, lane 4 versus lane 2).

Collectively, these results show that the presence of profurin leads to ApoB degradation in proteasomes without affecting ApoB transcription, and thus reduces VLDL secretion.

Hepatic profurin overexpression did not result in lipid accumulation in livers of *Ldlr*^{-/-} mice

To determine whether reduced VLDL secretion due to profurin treatment resulted in liver lipid accumulation, a common side effect of blockage of VLDL secretion in mice by other means¹⁹, the livers of *Ldlr*^{-/-} mice fed a Western diet were examined on day 28 after Ad-profurin or Ad-null transduction. Liver TC and TG levels did not differ between the two groups (Fig. S3, A and B). Histological analysis by H&E staining of liver sections revealed no gross abnormalities in the Ad-profurin compared with the Ad-null group (Fig. S3C). Oil-red O staining showed a similar distribution of lipid droplets in both groups (Fig. S3D). To further evaluate the acute effect of profurin on liver status, we measured liver lipids and plasma alanine transaminase on day 3 after transduction when profurin is highly expressed. No differences were observed between the Ad-profurin and Ad-null groups in plasma alanine transaminase, liver TC or TG levels (Fig. S4). Thus, short-term hepatic profurin expression did not cause liver damage or lipid accumulation.

Profurin overexpression attenuates vascular injury

To determine if profurin has a vasculoprotective effect in injury models not involving sub-endothelial lipid accumulation, WT mice were infused with Ad-null or Ad-profurin and immediately subjected to intraluminal artery injury. A wire was inserted into the femoral artery and the end used to scrape and hence disrupt the inner lumen of the vessel¹³. Profurin transduction significantly reduced the subsequent wall thickening induced by wire injury relative to that of Ad-null control mice (Fig. 7A). We also implemented a non-denuding injury to the vasculature using the common carotid ligation model¹³. While overexpression

of profurin had no effect on naïve common carotid arteries (Fig. 7B), it significantly reduced the subsequent wall thickening caused by common carotid artery ligation (Fig. 7C). Further, VSMCs were isolated from WT mice to determine if subsequent profurin overexpression would reduce cell proliferation. Prolurin decreased native furin protein amounts in the VSMCs (Fig. 8A). BrdU incorporation, an index of cell proliferation, was reduced by profurin treatment (Fig. 8B), as was cell migration (Fig. 8C and D). Consistent with an inhibitory effect on vascular injury and cell proliferation, cell cycle analysis revealed a reduction in the number of cells in the synthesis phase when cells were exposed to Ad-profurin (Fig. 8E).

Together, when expressed in VSMCs *in vitro*, profurin inhibited proliferation and migration, and thus may contribute to its vasuloprotective effects in models of either wire-induced femoral artery injury or common carotid artery ligation.

Discussion and Conclusions

Previously we reported that hepatic overexpression of profurin lowered HDL-c levels and reduced reverse cholesterol transport in WT mice ⁶, potentially negative effects for arterial health. Here we show that, despite this, hepatic profurin overexpression results in a significant reduction in atherosclerotic lesion development in *Ldlr*^{-/-} mice (Fig. 1).

One of the surprising findings is that hepatic profurin overexpression reduces plasma ApoB-containing lipoprotein cholesterol levels (Figs. 3 and 4). Because the *Ldlr*^{-/-} mouse model was used, the effect is not dependent on the LDLR, indicating that a profurin-based drug could be used in combination with statins to lower LDL-c levels. In addition, we observed a similar effect of hepatic profurin overexpression in ApoE^{-/-} mouse (profurin, 242±65 versus control, 550±45 mg/dl, n=4, p<0.01).

Can the LDL-lowering effect of profurin alone explain profurin's protective effect against lesion formation? The LDL-lowering effect of profurin after vector-mediated gene transfer probably does not extend longer than 3 weeks. However, abundant previous work indicates that even a few weeks reduction of LDL-c has significant effects on lesion formation²⁰⁻²². This supports the likelihood of a major role for the reduced LDL levels in bringing about our encouraging lesion results after profurin overexpression. In the current study, transduction results are transient so that the maximum effect of profurin on the progression of atherosclerosis could not be realized. Likewise, further work is needed to confirm that there are no deleterious effects of long-term profurin overexpression on the liver. We are currently developing transgenic mice expressing profurin in the liver to address these topics.

The detailed molecular mechanism(s) by which profurin affects ApoB-containing lipoprotein metabolism is not fully understood. The fact that profurin is overexpressed in the liver indicates that hepatic factors are involved. This study clearly shows that hepatic profurin overexpression leads to apoB degradation via the proteosomes, which reduces VLDL secretion (Fig. 6). This effect is quite different from what is known about how endothelial lipase controls ApoB-containing lipoproteins clearance²³ and warrants further investigation. Since furin is not known to regulate VLDL secretion, it is possible that hepatic

profurin overexpression may reduce VLDL secretion independently of any effect of furin. Importantly, blocking VLDL secretion often results in hepatic lipid accumulation¹⁹, however, in this study, short-term hepatic profurin overexpression does not have this effect.

PCSK9 is a recently identified hepatic modulator of plasma ApoB-containing lipoproteins acting by accelerating LDLR degradation²⁴. Does profurin affect the function of this atypical TPC? Seidah and associates have shown that PCSK9 is cleaved by furin *in vitro*²⁵ and *in vivo*²⁶, and that this decreases PCSK9 function. Thus, hepatic overexpression of profurin could potentially influence the processing of PCSK9 through inhibition of the activity of furin. Interestingly, a deficiency of PCSK5 in some unknown way increases PCSK9 cleavage²⁶. In theory, profurin should block both furin and PCSK5 activities. Thus, the net effect of profurin on PCSK9 processing is likely to be minimal, if any. We believe that the LDL-lowering effect of profurin in *Ldlr*^{-/-} mice is unlikely to be mediated by PCSK9 since profurin is effective in *Ldlr*^{-/-} mice where PCSK9 cannot exert an LDLR-requiring function. Future experiments are needed to determine the relative contribution of the profurin-furin-PCSK9 pathway to plasma ApoB metabolism in mouse models different from the *Ldlr*^{-/-} and/or *pcsk9*^{-/-} mice.

We have demonstrated that profurin has vasculoprotective effects not only against classical sub-endothelial lipid accumulation but also in the attenuation of the vascular remodeling that occurs in both the wire injury and ligation injury models. There are several possible mechanisms: (i) adenoviral vector encoding profurin may infect vascular cells locally when the integrity of the vessel is compromised. Although the adenoviral vector is known to poorly transduce intact vessels, Klugherz *et al* reported significant delivery of vector in smooth muscle cells after the local arterial wall were expanded with balloon stents²⁷. Further studies will be required to determine if there are cells expressing profurin in the injured vascular wall; (ii) profurin may alter the secretion of hepatic-derived factors that affect vascular remodeling, since there are many potential TPCs' substrates in the liver; and/or (iii) the effect is due to decreased plasma cholesterol levels. There is substantial supporting evidence for the last: hypercholesterolemic mice, produced by either diet or targeted disruption of the lipid uptake mechanism, exhibit excessive remodeling in response to vascular injury²⁸⁻³¹. Further studies are required to evaluate these mechanisms.

The "proof of concept" experiments presented here clearly demonstrate that profurin overexpression increases hepatic apoB degradation, decreases VLDL secretion, lowers plasma atherogenic lipoproteins and significantly reduces progression of atherosclerosis in mice. In addition, profurin reduces pathological vascular remodeling. The results provide a platform for exploration of profurin-based therapeutic strategies which target LDL-c and function independently of the LDLR.

Supplementary Material

Refer to Web version on PubMed Central for supplementary material.

Acknowledgments

This work was supported by grant HL081861 and HL08186104S1 (W.J.) from the National Heart Lung and Blood Institute. We are indebted to Ms Afroza Huq for her excellent technical assistance and thank Drs. Julie Rushbrook and M.M. Hussain for their critical reading and comments.

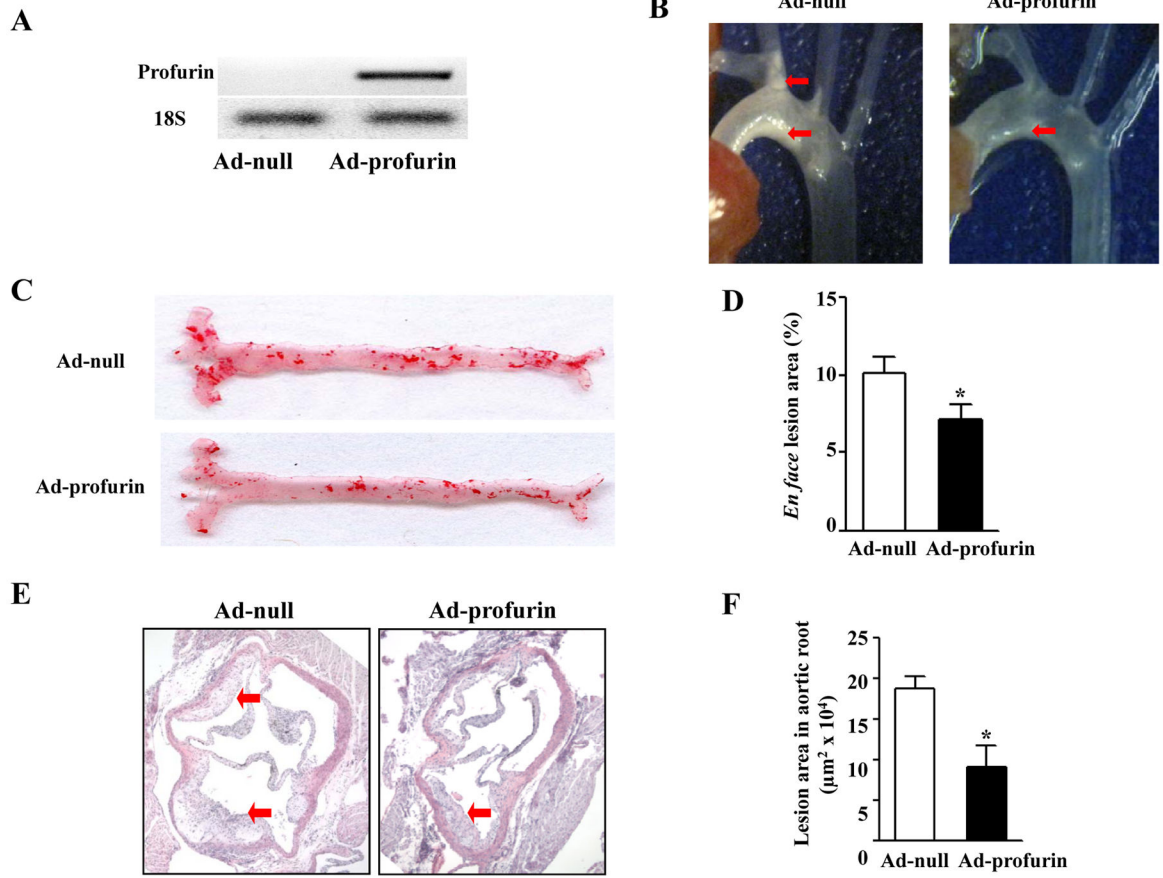
References

1. Seidah NG, Chretien M. Proprotein and prohormone convertases: a family of subtilases generating diverse bioactive polypeptides. *Brain Res.* 1999; 848:45–62. [PubMed: 10701998]
2. Seidah NG, Sadr MS, Chretien M, et al. The multifaceted Proprotein Convertases: their unique, redundant, complementary and opposite functions. *J Biol Chem.* 2013
3. Seidah NG, Khatib AM, Prat A. The proprotein convertases and their implication in sterol and/or lipid metabolism. *Biol Chem.* 2006; 387:871–877. [PubMed: 16913836]
4. Thomas G. Furin at the cutting edge: from protein traffic to embryogenesis and disease. *Nat Rev Mol Cell Biol.* 2002; 3:753–766. [PubMed: 12360192]
5. Zhong M, Munzer JS, Basak A, et al. The prosegments of furin and PC7 as potent inhibitors of proprotein convertases. In vitro and ex vivo assessment of their efficacy and selectivity. *J Biol Chem.* 1999; 274:33913–33920. [PubMed: 10567353]
6. Jin W, Wang X, Millar JS, et al. Hepatic proprotein convertases modulate HDL metabolism. *Cell Metab.* 2007; 6:129–136. [PubMed: 17681148]
7. Stawowy P, Kallisch H, Borges Pereira Stawowy N, et al. Immunohistochemical localization of subtilisin/kexin-like proprotein convertases in human atherosclerosis. *Virchows Arch.* 2005; 446:351–359. [PubMed: 15756593]
8. Lei X, Shi F, Basu D, et al. Proteolytic processing of angiopoietin-like protein 4 by proprotein convertases modulates its inhibitory effects on lipoprotein lipase activity. *J Biol Chem.* 2011; 286:15747–15756. [PubMed: 21398697]
9. Liu J, Huan C, Chakraborty M, et al. Macrophage sphingomyelin synthase 2 deficiency decreases atherosclerosis in mice. *Circ Res.* 2009; 105:295–303. [PubMed: 19590047]
10. Folch J, Lees M, Sloane Stanley GH. A simple method for the isolation and purification of total lipides from animal tissues. *J Biol Chem.* 1957; 226:497–509. [PubMed: 13428781]
11. Yazdanyar A, Jiang XC. Liver phospholipid transfer protein (PLTP) expression with a PLTP-null background promotes very low-density lipoprotein production in mice. *Hepatology.* 2012; 56:576–584. [PubMed: 22367708]
12. Chakraborty M, Lou C, Huan C, et al. Myeloid cell-specific serine palmitoyltransferase subunit 2 haploinsufficiency reduces murine atherosclerosis. *J Clin Invest.* 2013; 123:1784–1797. [PubMed: 23549085]
13. Anea CB, Zhang M, Stepp DW, et al. Vascular disease in mice with a dysfunctional circadian clock. *Circulation.* 2009; 119:1510–1517. [PubMed: 19273720]
14. Jin W, Fuki IV, Seidah NG, et al. Proprotein convertases [corrected] are responsible for proteolysis and inactivation of endothelial lipase. *J Biol Chem.* 2005; 280:36551–36559. [PubMed: 16109723]
15. Anea CB, Ali MI, Osmond JM, et al. Matrix metalloproteinase 2 and 9 dysfunction underlie vascular stiffness in circadian clock mutant mice. *Arterioscler Thromb Vasc Biol.* 2010; 30:2535–2543. [PubMed: 20829506]
16. Wolfrum C, Poy MN, Stoffel M. Apolipoprotein M is required for prebeta-HDL formation and cholesterol efflux to HDL and protects against atherosclerosis. *Nat Med.* 2005; 11:418–422. [PubMed: 15793583]
17. Broedl UC, Jin W, Fuki IV, et al. Structural basis of endothelial lipase tropism for HDL. *FASEB J.* 2004; 18:1891–1893. [PubMed: 15456739]
18. Millar JS, Cromley DA, McCoy MG, et al. Determining hepatic triglyceride production in mice: comparison of poloxamer 407 with Triton WR-1339. *J Lipid Res.* 2005; 46:2023–2028. [PubMed: 15995182]

19. Raabe M, Flynn LM, Zlot CH, et al. Knockout of the abetalipoproteinemia gene in mice: reduced lipoprotein secretion in heterozygotes and embryonic lethality in homozygotes. *Proc Natl Acad Sci U S A*. 1998; 95:8686–8691. [PubMed: 9671739]
20. Nakajima K, Yamashita T, Kita T, et al. Orally administered eicosapentaenoic acid induces rapid regression of atherosclerosis via modulating the phenotype of dendritic cells in LDL receptor-deficient mice. *Arterioscler Thromb Vasc Biol*. 2011; 31:1963–1972. [PubMed: 21817104]
21. Parathath S, Grauer L, Huang LS, et al. Diabetes adversely affects macrophages during atherosclerotic plaque regression in mice. *Diabetes*. 2011; 60:1759–1769. [PubMed: 21562077]
22. Van Craeyveld E, Gordts SC, Nefyodova E, et al. Regression and stabilization of advanced murine atherosclerotic lesions: a comparison of LDL lowering and HDL raising gene transfer strategies. *J Mol Med (Berl)*. 2011; 89:555–567. [PubMed: 21249329]
23. Broedl UC, Maugeais C, Millar JS, et al. Endothelial lipase promotes the catabolism of ApoB-containing lipoproteins. *Circulation research*. 2004; 94:1554–1561. [PubMed: 15117821]
24. Denis M, Marcinkiewicz J, Zaid A, et al. Gene inactivation of proprotein convertase subtilisin/kexin type 9 reduces atherosclerosis in mice. *Circulation*. 2012; 125:894–901. [PubMed: 22261195]
25. Benjannet S, Rhoads D, Hamelin J, et al. The proprotein convertase (PC) PCSK9 is inactivated by furin and/or PC5/6A: functional consequences of natural mutations and post-translational modifications. *J Biol Chem*. 2006; 281:30561–30572. [PubMed: 16912035]
26. Essalmani R, Susan-Resiga D, Chamberland A, et al. In vivo evidence that furin from hepatocytes inactivates PCSK9. *J Biol Chem*. 2011; 286:4257–4263. [PubMed: 21147780]
27. Klugherz BD, Song C, DeFelice S, et al. Gene delivery to pig coronary arteries from stents carrying antibody-tethered adenovirus. *Human gene therapy*. 2002; 13:443–454. [PubMed: 11860711]
28. Oguchi S, Dimayuga P, Zhu J, et al. Monoclonal antibody against vascular cell adhesion molecule-1 inhibits neointimal formation after periadventitial carotid artery injury in genetically hypercholesterolemic mice. *Arterioscler Thromb Vasc Biol*. 2000; 20:1729–1736. [PubMed: 10894810]
29. Reis ED, Roque M, Dansky H, et al. Sulindac inhibits neointimal formation after arterial injury in wild-type and apolipoprotein E-deficient mice. *Proc Natl Acad Sci U S A*. 2000; 97:12764–12769. [PubMed: 11027305]
30. Tacke PJ, Delsing DJ, Gijbels MJ, et al. VLDL receptor deficiency enhances intimal thickening after vascular injury but does not affect atherosclerotic lesion area. *Atherosclerosis*. 2002; 162:103–110. [PubMed: 11947903]
31. Zhu B, Kuhel DG, Witte DP, et al. Apolipoprotein E inhibits neointimal hyperplasia after arterial injury in mice. *Am J Pathol*. 2000; 157:1839–1848. [PubMed: 11106557]

Highlights

- Hepatic profurin overexpression prevents lesion development in *ldlr*^{-/-} mice.
- Profurin overexpression induces hepatic apoB degradation in the proteasomes.
- Profurin overexpression decreases VLDL secretion.
- Short-term hepatic profurin expression does not result in liver lipid accumulation.
- Profurin has vasculoprotective effects on pathological vascular remodeling.



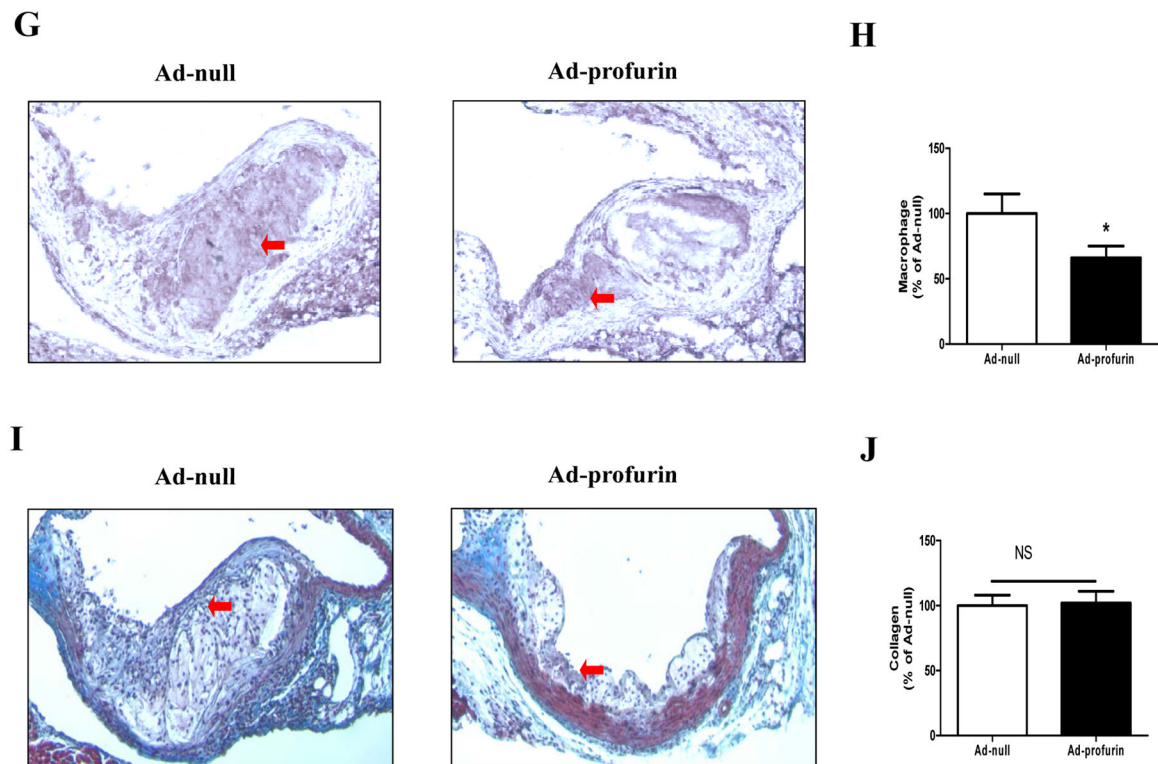


Fig. 1. Hepatic profurin overexpression decreased lesion progression in *Ldlr*^{-/-} mice fed a Western diet. Liver profurin mRNA was analyzed in mice sacrificed on day 28 after transduction. (A). The remaining studies were also carried out on mice sacrificed on day 28. In Ad-null and Ad-profurin mice, the dissected aortic arch area was photographed (B), lipid accumulation in the aorta was detected by *en face* staining with Oil Red O (C), and the lesion area of the aorta quantified as a % of the total aorta area (D). Hematoxylin and eosin staining of the cross sections of the proximal aorta in the root assay were carried out as described in the Methods section (E) and the lesion area was quantified (F). The images shown in B, C and E are representative. Atherosclerotic lesions are indicated by arrows in B and E. The cross sections of the proximal aorta were used for immunohistochemical staining of macrophages (G) and the Masson trichrome staining for collagen (I). The macrophage content and collagen positive area were quantified and compared, respectively in H and J. The images shown in A, C, G and H are representative. Data are presented as mean ± SD, n = 11 mice per group, * $P < 0.05$, ** $P < 0.01$.

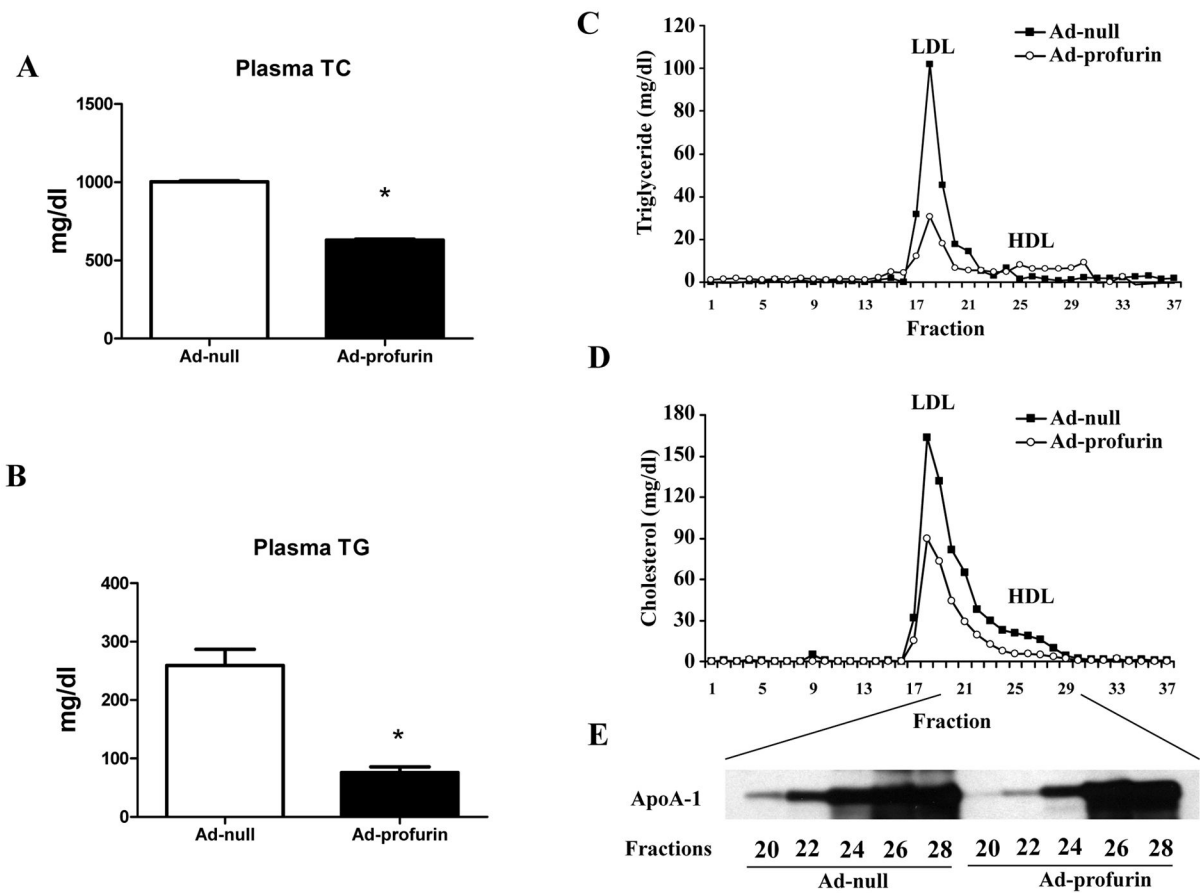


Fig. 2. Plasma TC and TG levels in *Ldlr*^{-/-} mice on a Western diet after hepatic profurin over-expression. *Ldlr*^{-/-} mice fed a Western diet were injected with Ad-null or Ad-profurin via the tail vein. Plasma TC (A) and TG (B) were measured on day 3 after injection. Data are presented as mean ± SD, n = 11 per group, ** *P* < 0.01. The TG (C) and TC (D) levels in LDL and HDL fractions were determined on day 3 following separation of plasma lipoproteins by FPLC. Mouse ApoA-1 expression in the indicated fractions was determined by immunoblotting (E). Signals in fractions 26 and 28 were saturated for both groups.

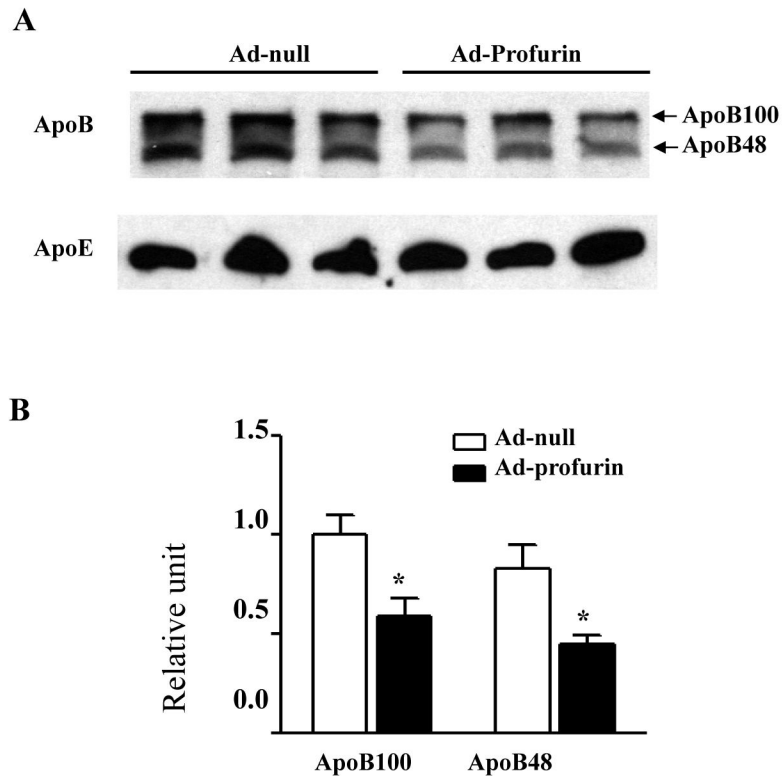


Fig. 3. Plasma ApoB and ApoE levels in the day 3 *Ldlr*^{-/-} mice on a Western diet. Plasma ApoB100, ApoB48 and ApoE were detected by Western blotting in both control and profurin-treated groups (A), and ApoB 100 and 48 quantified (B). Data are presented as mean ± SD, n =3 per group, * *P* < 0.05.

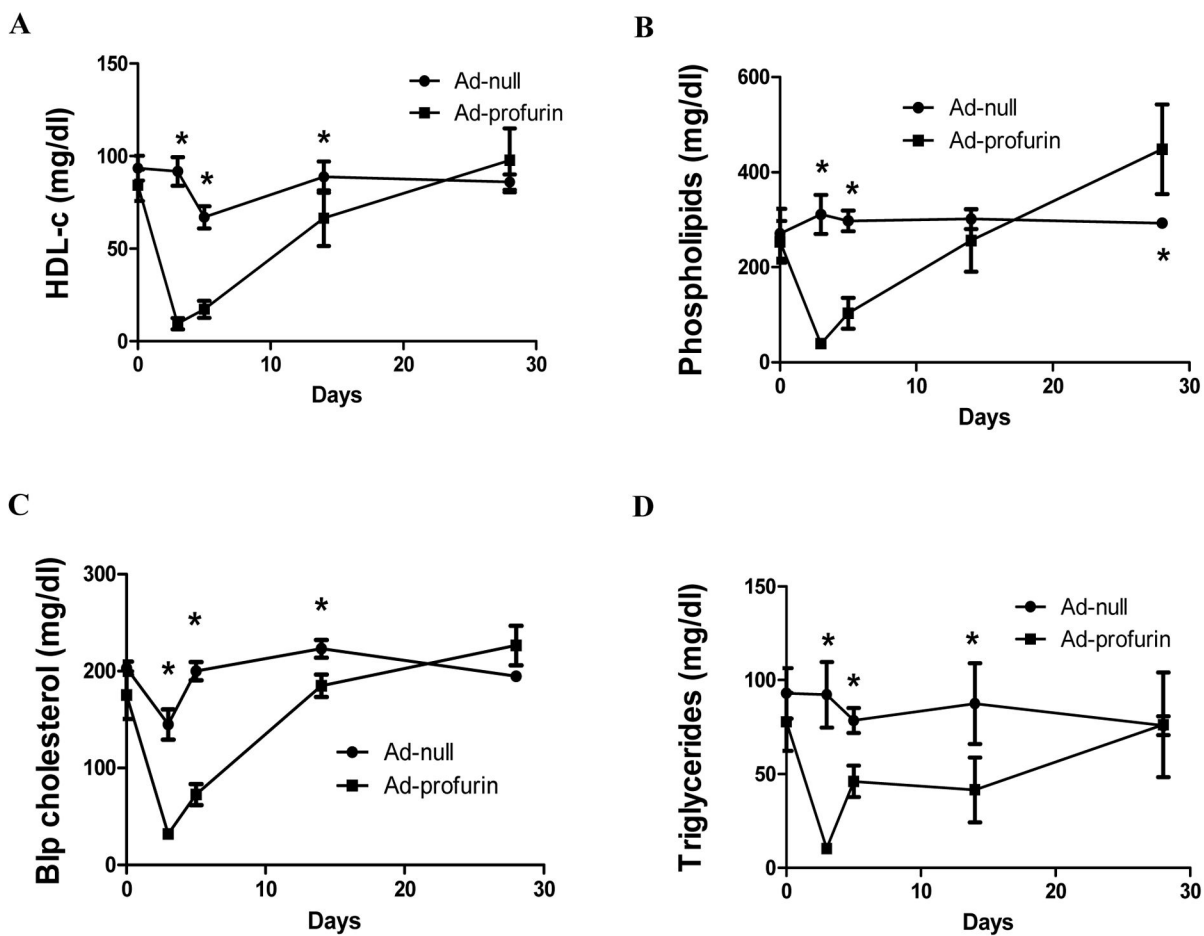


Fig. 4. Characterization of plasma lipids in *Ldlr*^{-/-} mice after hepatic profurin over-expression. *Ldlr*^{-/-} mice fed a chow diet were injected with Ad-null or Ad-profurin via the tail vein. Plasma samples were collected on days 0, 3, 5, 14 and 28. HDL-c (A), phospholipids (B), ApoB-containing lipoprotein cholesterol (C) and TG (D) were measured. Data are presented as the mean ± SD, n =4 per group, * *P* < 0.05.

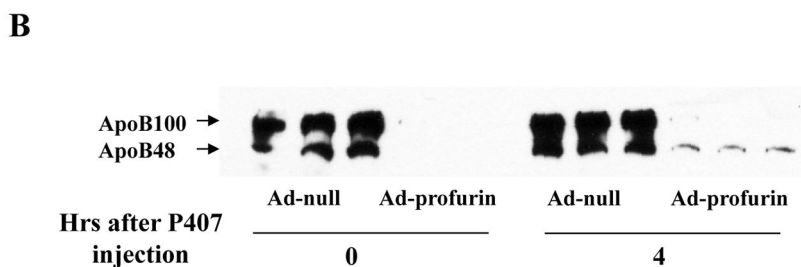
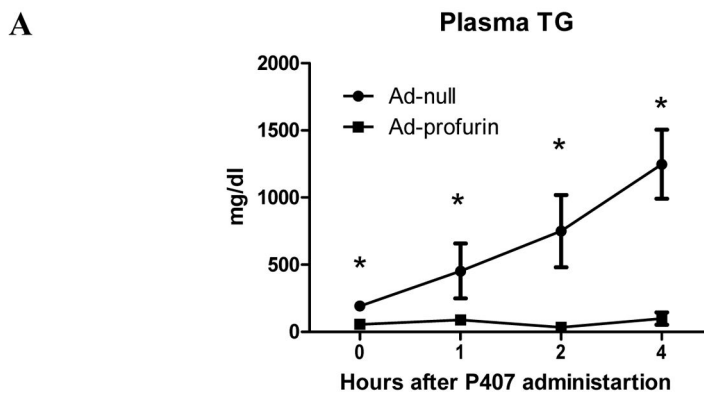


Fig. 5. VLDL secretion after hepatic profurin over-expression on a chow diet. *Ldlr*^{-/-} mice fed a chow diet were injected with Ad-null or Ad-profurin via the tail vein. On day 3 after transduction, overnight fasted mice were injected intraperitoneally with P407 (1mg/kg). Blood samples were collected at the indicated time points. Plasma TG levels and ApoB proteins were determined as described in Methods. Data are presented as the mean ± SD, n =4 per group for TG levels, 3 per group for ApoB proteins, * *P* < 0.01.

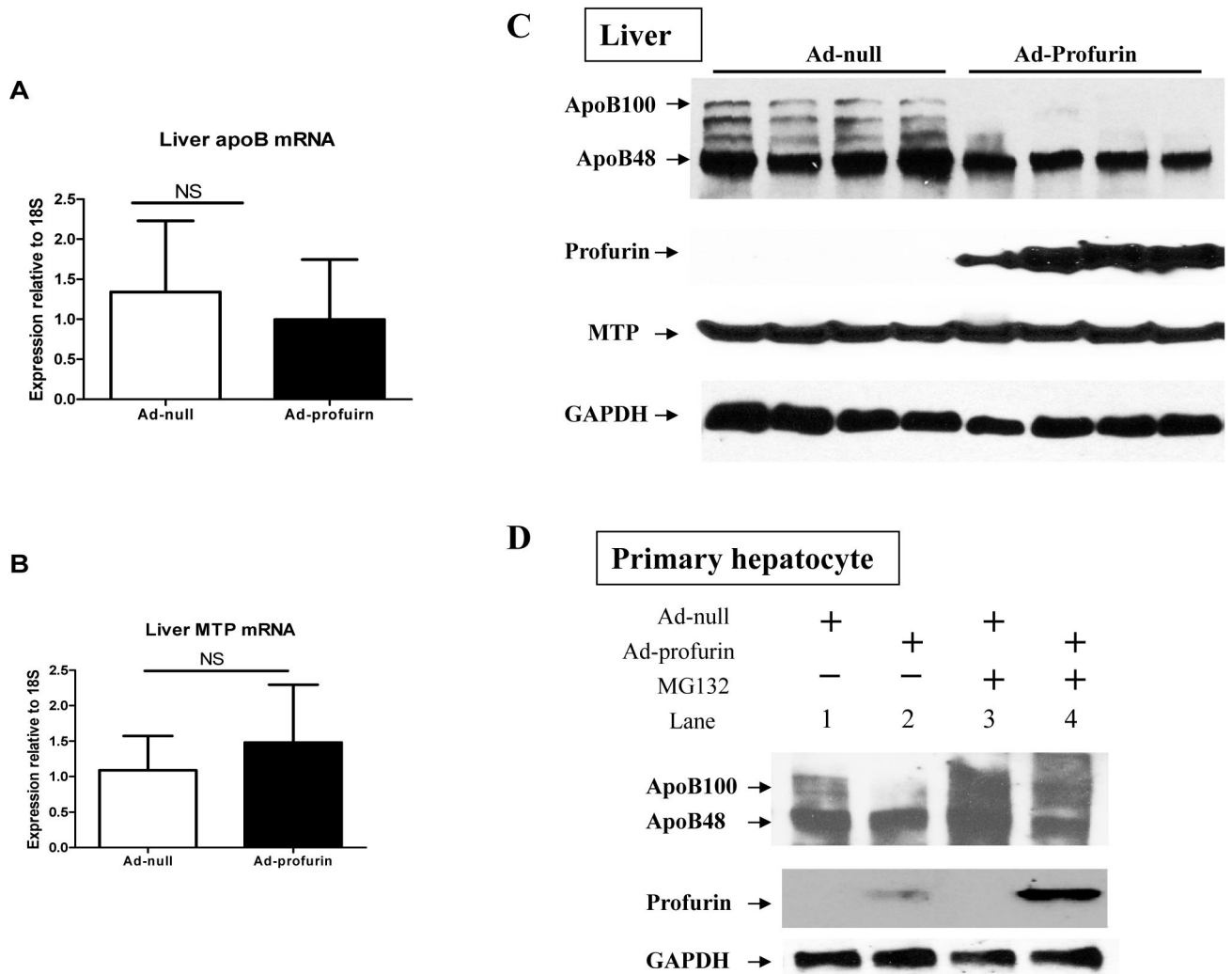


Fig. 6. Liver/hepatocyte mRNA and protein analysis. Eight week old *Ldlr*^{-/-} mice on a chow diet were injected with Ad-null or Ad-profurin, sacrificed on day 3 and the livers collected. (A) apoB mRNA; (B) MTP mRNA. Data are presented as mean ± SD, n =4 mice per group. NS: not significant. (C) Western blot analysis of liver protein levels; Primary hepatocytes were infected with either Ad-null or Ad-profurin. Cells were treated with either DMSO or MG132 overnight. Cell lysates were prepared as described in MATERIALS & METHODS. (D) Western blot analysis of indicated proteins in the cell lysates.

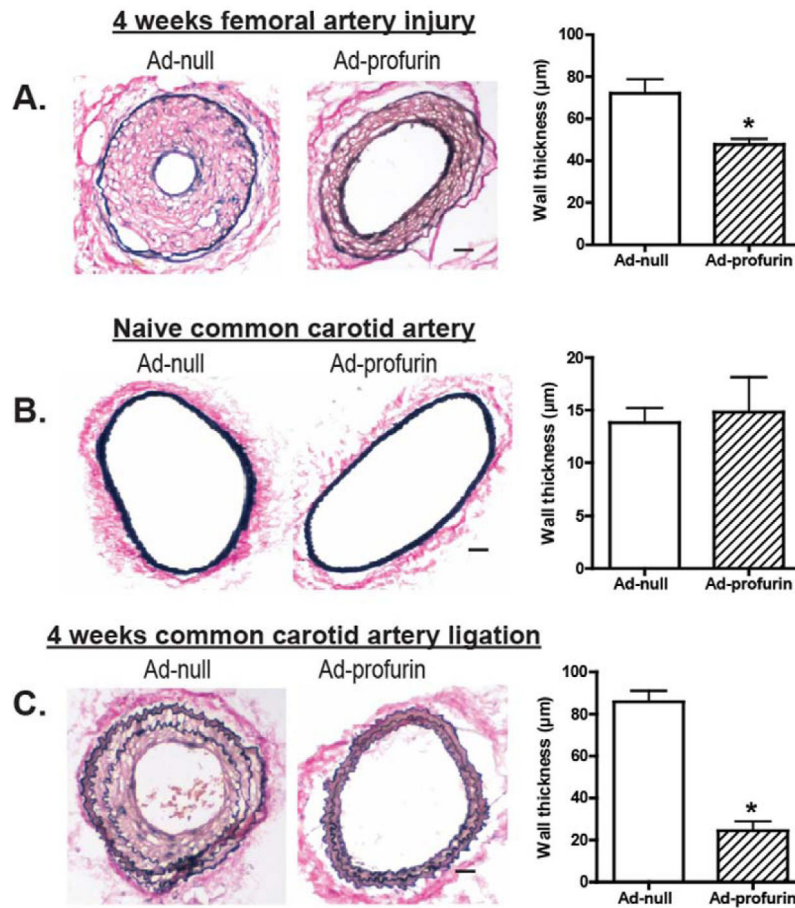


Fig. 7. Vascular injury in WT mice is reduced by profurin overexpression. WT mice were injected with Ad-null or Ad-profurin and subsequently subjected to vascular injury. (A) A denuding endothelial injury was induced by inserting a wire into the femoral artery and systematically disrupting the inner lumen of the vessel. Four weeks later, mice were euthanized, the femoral artery was isolated, artery cross sections were visualized by von Gieson staining (left panel). Wall thickness was measured and compared (right panel). A non-denuding vascular injury was performed by ligating the common carotid artery. Four weeks later, histomorphometric analysis was performed on naïve uninjured right common carotid arteries (B), and ligated left common carotid arteries (C) from each group. Data are presented as the mean \pm SD, $n=5$, * $P < 0.05$.

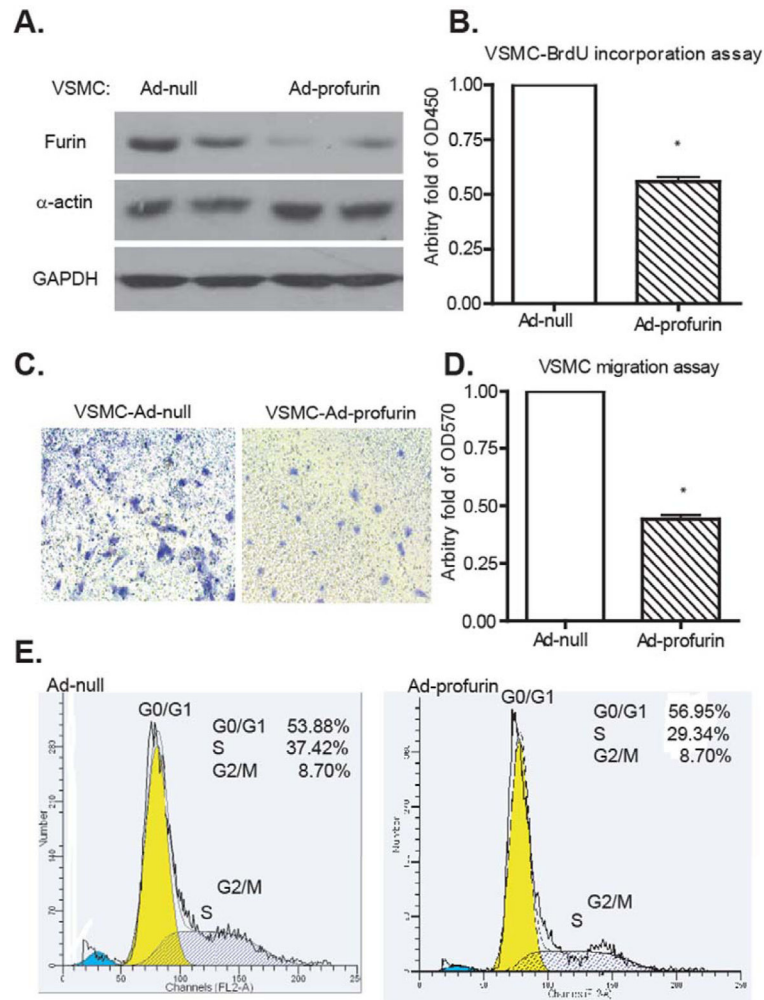


Fig. 8. Profurin suppresses vascular smooth muscle cell proliferation and migration. VSMCs were isolated from WT mice and transduced with either Ad-null or Ad-profurin. (A) Protein lysates from VSMCs positive for α -actin detected by Western blotting revealed that Ad-profurin reduced furin expression (N=3). (B) VSMCs isolated from WT mice were transduced with the adenoviral vectors and after 48 hours treated with 25 ng/mL PDGF and 10 μ m BrdU. Ad-profurin expressing VSMCs exhibited decreased BrdU incorporation relative to Ad-null expressing cells. (C) For cell migration, VSMCs were plated on Transwell filters coated with fibronectin and stimulated again with 25 ng/mL PDGF. After 4 hours, the cells that migrated to the lower filter compartment were fixed and stained with crystal violet and quantified by spectrophotometry at 570 nm (D). VSMCs transduced with either Ad-null or Ad-profurin were incubated with 25ng/mL PDGF for 24 hours, trypsinized, and stained with propidium iodide and analyzed by FACS (E).